Vitreous M2 Macrophage-Derived Microparticles Promote RPE Cell Proliferation and Migration in Traumatic Proliferative Vitreoretinopathy

Yinting Song,[1] Mengyu Liao,[1] Xiao Zhao,[1] Han Han,[1] Xue Dong,[1,2] Xiaohong Wang,[2] Mei Du,[2] and Hua Yan[1,2]

[1]Department of Ophthalmology, Tianjin Medical University General Hospital, Tianjin, China
[2]Laboratory of Molecular Ophthalmology, Department of Pharmacology and Tianjin Key Laboratory of Inflammation Biology, School of Basic Medical Sciences, Tianjin Medical University, Tianjin, China

Correspondence: Hua Yan, Department of Ophthalmology, Tianjin Medical University General Hospital, No. 154 Anshan Road, Tianjin 300052, China; zyyyanhua@tmu.edu.cn.
Mei Du, Laboratory of Molecular Ophthalmology, Department of Pharmacology and Tianjin Key Laboratory of Inflammation Biology, School of Basic Medical Sciences, Tianjin Medical University, No. 22 Qixiangtai Road, Tianjin 300070, China; dumei@tmu.edu.cn.

YS and ML contributed equally to this work.

Received: December 13, 2020
Accepted: September 7, 2021
Published: September 23, 2021

Citation: Song Y, Liao M, Zhao X, et al. Vitreous M2 macrophage-derived microparticles promote RPE cell proliferation and migration in traumatic proliferative vitreoretinopathy. *Invest Ophthalmol Vis Sci.* 2021;62(12):26. https://doi.org/10.1167/iovs.62.12.26

Purpose. To characterize vitreous microparticles (MPs) in patients with traumatic proliferative vitreoretinopathy (PVR) and investigate their role in PVR pathogenesis.

Methods. Vitreous MPs were characterized in patients with traumatic PVR, patients with rhegmatogenous retinal detachment (RRD) complicated with PVR, and control subjects by flow cytometry. The presence of M2 macrophages in epiretinal membranes was measured by immunostaining. Vitreous cytokines were quantified by ELISA assay. For in vitro studies, MPs isolated from THP-1 cell differentiated M1 and M2 macrophages, termed M1-MPs and M2-MPs, were used. The effects and mechanisms of M1-MPs and M2-MPs on RPE cell proliferation, migration, and epithelial to mesenchymal transition were analyzed.

Results. Vitreous MPs derived from photoreceptors, microglia, and macrophages were significantly increased in patients with traumatic PVR in comparison with control and patients with RRD (PVR), whereas no significance was identified between the two control groups. M2 macrophages were present in epiretinal membranes, and their signature cytokines were markedly elevated in the vitreous of patients with traumatic PVR. Moreover, MPs from M2 macrophages were increased in the vitreous of patients with traumatic PVR. In vitro analyses showed that M2-MPs promoted the proliferation and migration of RPE cells via activation of the phosphatidylinositol 3-kinase (PI3K)/protein kinase B (AKT)/mammalian target of rapamycin (mTOR) signaling pathway. However, M2-MPs did not induce the expression of fibrotic proteins, including fibronectin, α-smooth muscle actin, and N-cadherin in RPE cells.

Conclusions. This study demonstrated increased MP shedding in the vitreous of patients with traumatic PVR; specifically, MPs derived from M2 polarized macrophages may contribute to PVR progression by stimulating RPE cell proliferation and migration.

Keywords: proliferative vitreoretinopathy, ocular trauma, vitreous microparticles, PI3K/AKT/mTOR signaling pathway

Proliferative vitreoretinopathy (PVR) is a common challenging complication of open globe injuries and rhegmatogenous retinal detachment (RRD), which occurs in 40% to 60% of patients with open globe injuries and 8% to 10% of patients with RRD.[1,2] Eyes with PVR often progress to tractional retinal detachment, which is the most common cause of surgical failure for RRD and open globe injuries.[3] The pathogenesis of PVR is complex and involves the following stages: breakdown of the blood–retinal barrier, chemotaxis and cellular migration, cellular proliferation, membrane formation with the remodeling of the extracellular matrix, and contraction.[4–6] RPE cells are present in almost 100% of epiretinal membranes and are considered the prominent participants in PVR progression.[1,2,7] However, the mechanism underlying the activation and epithelial-to-mesenchymal transition (EMT) of RPE cells remains elusive.

Microparticles (MPs) are submicron vesicles formed by budding and blebbing of cell membranes.[8] They range from 100 nm to 1000 nm in size and express specific markers of parental cells, which can be used to determine their cellular origin. MPs can be released during various cellular activities, including cell activation or cell injury, or following cell senescence and apoptosis.[9,10] Numerous studies have revealed the biological activities of MPs in cell adhesion, apoptosis, vascular function, and angiogenesis.[11–15] MPs have been identified in human plasma and other tissue compartments such as synovial fluid,[11–13] and increased levels of circulating MPs are associated with various diseases.[13–15] In the eye, elevated vitreous MPs have been reported for patients with proliferative diabetic retinopathy and RRD, and their increased amount stimulates endothelial proliferation and angiogenesis in vitro.[16,17]

Ocular trauma is associated with vitreous hemorrhage and significant damage of ocular structures and retinal cells, indicating that vitreous MPs might be increased locally from injured retinal cells or from blood origin. Nevertheless, the pathobiological roles of MPs in ocular trauma remain to be determined.

Macrophages are cellular components of PVR membranes, and they migrate into the vitreous during vitreous hemorrhage and retinal break, suggesting that macrophages might contribute to the development of intraocular proliferation and fibrosis.[18,19] Macrophages can be phenotypically characterized as M1 and M2 subtypes, with M1 macrophages being proinflammatory and M2 macrophages playing a significant role in wound healing and tissue remodeling.[20,21] Macrophage-derived extracellular vesicles have been detected in body fluid and tissues, where they function as critical regulators of cross-talk between macrophages and surrounding tissue, thereby modulating the migratory and proliferative properties of target cells.[22,23]

In this study, we analyzed vitreous MPs from different cell origins in patients with open globe injuries who developed PVR, and we also investigated the potential effects of M2 macrophage-derived MPs on activation of RPE cells in vitro.

Materials and Methods

Collection of Vitreous Samples From Human Patients

Seventy-two patients who underwent vitrectomy in the ophthalmology department of Tianjin Medical University General Hospital between June 2016 and December 2018 were included. Vitreous samples were collected during the standardized three-port vitrectomy for the treatment of retinal diseases. Specifically, vitreous samples were collected from 27 eyes of RRD complicated with PVR, including two eyes with concomitant idiopathic macular hole, 15 eyes with traumatic PVR, and 31 eyes of 30 patients with idiopathic macular hole, idiopathic epiretinal membrane, or ectopia lentis as controls. The demographic characteristics of the patients are summarized in the Table.

The exclusion criteria included previous laser coagulation within the last 3 months, malignant tumors, and any other ocular condition such as glaucoma or diabetic retinopathy. In this study, the diagnosis of traumatic PVR was based on the criteria proposed by the Retina Society Terminology Committee.[24] This study was reviewed and approved by the ethics committees of Tianjin Medical University and adhered to the tenets of the Declaration of Helsinki. All patients gave written informed consent.

Isolation and Identification of Microparticles

MPs were isolated by density gradient ultracentrifugation as described previously.[25–27] Briefly, human vitreous samples or THP-1 cell culture medium were centrifuged at 4400*g* for 15 minutes and at 13,000*g* for 2 minutes at 4°C to remove cells and debris. MPs in the supernatant were further purified by centrifugation at 20,000*g* for 90 minutes, then MPs were resuspended in PBS and stored at –80°C until use. The ultrastructure of isolated MPs was examined under a transmission electron microscope (HT7700; Hitachi, Tokyo, Japan) at the Research Centre of Basic Medical Science of Tianjin Medical University. The size distribution of MPs was determined by nanoparticle tracking analysis (NS300; Malvern Panalytical, Malvern, UK).

Flow Cytometry

Analysis of vitreous MPs by flow cytometry was performed on an LSRFortessa flow cytometer (Becton, Dickinson and Company, Franklin Lakes, NJ, USA) and was analyzed using FlowJo. A mix of 0.5-, 0.9-, and 3.0-µm BioCytex beads (BioCytex SARL, Marseille, France) was used to set up an acquisition gate to include particles measuring up to 0.9 µm in diameter. Vitreous samples were run on the same setting to identify particles within the gate (including all particles of ≤1 µm in size). Retinal-derived MPs were labeled with lectin from fluorescein isothiocyanate–labeled peanut agglutinin (FITC-PNA; Sigma-Aldrich, St. Louis, MO, USA) and lectin from fluorescein isothiocyanate–labeled isolectin B4 (FITC-ILB4; Sigma Aldrich).[17] D-Galactose (Sigma-Aldrich) served as isotype controls.[17] Macrophage-derived MPs were labeled with the CD14 antibody APC (BioLegend, San Diego, CA,

Table. Demographic and Clinical Characteristics of the Study Groups

	Control	PVR With RRD	Traumatic PVR
Patients/eyes, *n*	30/31	27/27	15/15
Sex (male/female), *n*	9/22	15/12	12/3*
Age (y), mean ± SD	63 ± 13	56 ± 15	42 ± 17*
Systemic diseases, *n* (%)			
Hypertension	11 (36)	8 (30)	5 (33)
Diabetes	3 (10)	5 (19)	1 (7)
Dyslipidemia	2 (7)	1 (4)	0 (0)
Coronary heart disease	2 (7)	2 (7)	0 (0)
Renal disease	1 (3)	0 (0)	1 (7)
Liver disease	0 (0)	1 (4)	0 (0)
Smoking, *n* (%)	4 (13)	4 (15)	4 (27)
Ophthalmology features, *n* (%)			
Epimacular membrane	1 (3)	0 (0)	0 (0)
Macular hole	29 (94)	2 (7)	1 (7)
Ectopia lentis	1 (3)	0 (0)	3 (20)
Proliferative vitreoretinopathy	0 (0)	27 (100)	15 (100)

* Significant difference between patients with traumatic PVR and control patients.

Investigative Ophthalmology & Visual Science

USA), and MPs expressing phosphatidylserine were labeled with PE Annexin V (BioLegend). Moreover, macrophage-derived MPs were further validated by dual-labeling with the CD14 antibody APC and the CD68 antibody PerCP (BioLegend). To determine the macrophage MP polarization states (M1 or M2 polarized macrophages), macrophage MPs were triple-labeled with the CD68 antibody PerCP, CD80 antibody PE (BioLegend), and CD163 antibody (BioLegend). Isotype-matched immunoglobulins (BioLegend) were used as controls. The concentration of MPs was calculated by comparison with calibrator beads of known concentration (Spherotech, Lake Forest, IL, USA).

Immunofluorescence

Fresh epiretinal membrane isolated from patients was fixed in 4% paraformaldehyde for 2 hours at room temperature and subsequently processed in 30% sucrose for 24 hours prior to embedding in optimal cutting temperature compound (Sakura Finetek Japan, Tokyo, Japan). The processed epiretinal membranes were cut into serial sections approximately 8 mm in size. The following antibodies were used in this study: anti–α-smooth muscle actin (αSMA; 1:200; Abcam, Cambridge, UK), anti-CD68 (1:100; Abcam), and anti-CD163 (1:200; Abcam). Slides were examined under a Zeiss fluorescent microscope (LSM 800; Carl Zeiss Microscopy, Jena, Germany).

For immunostaining assay, adult retinal pigment epithelial (ARPE)-19 cells were grown in 24-well cover glass to 80% confluence. After starvation overnight, ARPE-19 cells were treated with M1 macrophage MPs (M1-MPs) or M2 macrophage MPs (M2-MPs) for 48 hours. Cells were then fixed with 4% paraformaldehyde, permeabilized, and blocked with 2% BSA 0.3% Triton X-100/PBS. Cells were incubated with primary antibodies ZO-1 (1:50; Invitrogen, Waltham, MA, USA), fibronectin (1:100; Sigma-Aldrich), αSMA (1:100; Abcam), N-cadherin (1:100; Cell Signaling Technology, Danvers, MA, USA), or E-cadherin (1:80; ImmunoWay Biotechnology Company, Plano, TX, USA) overnight at 4°C, followed by incubation with secondary antibodies for 2 hours at room temperature. Images were acquired with a FV1000 confocal microscope (Olympus, Tokyo, Japan).

Measurement of Vitreous Cytokines

The concentrations of cytokines including interleukin (IL)-6, tumor necrosis factor (TNF)-α, monocyte chemoattractant protein (MCP)-1, IL-12, IL-10, and IL-1ra in human vitreous samples were measured by ELISA. In brief, ELISA kits were allowed to equilibrate at room temperature for 30 minutes prior to cytokine quantification according to the manufacturers' instruction. One ELISA kit (AMEKO, Shanghai, China) was used to measure soluble extracellular levels of IL-6 (D711013), TNF-α (D711045), MCP-1 (D711364), IL-12 (D711069), and IL-10 (D711114). Another ELISA kit (mlbio, Shanghai, China) was used to measure soluble extracellular levels of IL-1ra (ML058061).

Cell Culture

Human RPE cell line ARPE-19 (American Type Culture Collection, Manassas, VA, USA) was cultured in Gibco Dulbecco's modified Eagle's medium (DMEM)/F-12 medium (Thermo Fisher Scientific, Waltham, MA, USA) supplemented with Gibco 10% fetal bovine serum (FBS) and 1% penicillin–streptomycin. Human RPE cells were maintained at 37°C in a humidified atmosphere of 5% CO_2 and 95% air and grown to 80% to 90% confluence; passages 7 to 20 were used for the experiment. Before treatment with M1-MPs or M2-MPs for the indicated times and concentrations, cells were starved overnight with DMEM/F-12 containing 1% FBS.

Differentiation of THP-1 Cells

The human monocyte cell line THP-1 (American Type Culture Collection) was cultured in Gibco RPMI 1640 medium supplemented with 10% FBS and 1% penicillin–streptomycin at 37°C in 5% CO_2. Differentiation of THP-1 to M0 macrophages was induced by treatment with 320-nM phorbol 12-myristate 13-acetate (Sigma-Aldrich) for 24 hours. Afterward, cells were stimulated with either 1000 ng/mL lipopolysaccharide (LPS) and 20 ng/mL IFN-γ or 20 ng/mL IL-4 and 20 ng/mL IL-13 for 48 hours for induction of M1 or M2 polarized macrophages, respectively. The level of endotoxin contamination in M1-MPs was measured using an LPS ELISA kit (mlbio).

RNA Extraction and Real-Time Quantitative Polymerase Chain Reaction

To validate the successful differentiation of THP-1 cells into M1 or M2 polarized macrophages, the RNA of THP-1 cell–differentiated M1 or M2 macrophages was extracted using Trizol reagent (Life Technologies, Carlsbad, CA, USA), according to the manufacturer's protocol. RNA concentrations were measured with a NanoDrop One C spectrophotometer (Thermo Fisher Scientific). The quality of extracted RNA was detected by an ultraviolet spectrophotometer and further confirmed to be of good quality, with an A260/280 ratio of between 1.8 and 2.0 and A260/230 between 2.0 and 2.2. We used 1000 ng of total RNA to synthesize cDNA using the PrimeScript Reverse Transcription Reagent Kit (TransGen Biotech, Beijing, China). Real-time quantitative polymerase chain reaction (qRT-PCR) was performed in triplicate in a total volume of 20 µL containing 10 µL SYBR Green Master (Thermo Fisher Scientific), 1.2 µL PCR primers (at a final concentration of 0.3 mM), 1 µL cDNA template, and 7.8 µL of nuclease-free water. Amplifications were conducted using the CFX Connect system (Bio-Rad, Hercules, CA, USA) with the following cycle conditions: 95°C for 30 seconds, 40 cycles of 95°C for 5 seconds, and 60°C for 30 seconds. The expression levels of glyceraldehyde-3-phosphate dehydrogenase (GAPDH) were used as endogenous control. The sequences for the qRT-PCR primers are listed in Supplementary Table S1.

Cell Proliferation Assay

Cell Counting Kit 8 (CCK8; ApexBio, Houston, TX, USA) and bromodeoxyuridine (BrdU; Sigma-Aldrich) assays were employed to determine the effects of differentiated M1-MPs or M2-MPs from THP-1 cells on ARPE-19 cell proliferation. To determine the effects of vitreous MPs on RPE cell proliferation, MPs collected from three groups (control patients, patients with macular holes, and patients with traumatic PVR) were used for the CCK8 assay. For each group, vitreous samples from four randomly selected patients were pooled together as one biological replicate, and a total of three

Investigative Ophthalmology & Visual Science

replicates were used. MPs were isolated from the pooled vitreous samples as described above.

For the CCK8 assay, ARPE-19 cells were grown in a 96-well plate to 80% confluence. After treatment with MPs for 48 hours, cell proliferation was measured with the CCK8 kit. For the BrdU assay, ARPE-19 cells were starved overnight prior to treatment with M1-MPs or M2-MPs for 48 hours. BrdU (10 µM) was subsequently added and incubated for 4 hours at 37°C and detected with appropriate rat anti-BrdU (Abcam) and secondary antibody anti-rat Cy3 (Life Technologies). Nuclei were stained with 4′,6-diamidino-2-phenylindole (DAPI; Abcam), and images were taken using an Olympus FV1000 confocal microscope.

Cell Migration Assay

The effect of M1-MPs or M2-MPs on RPE cell migration was evaluated by wound healing and transwell assay. For the wound healing assay, ARPE-19 cells were grown in six-well plates to 80% confluence. After starvation overnight, the cell monolayers were scratched with 200 µL yellow tips and washed twice with PBS to remove the detached cells. Subsequently, cells were incubated with MPs for 48 hours at 37°C, and images were taken at 0, 24, and 48 hours after a scratch (Eclipse 80i; Nikon, Tokyo, Japan). To analyze cell migration, wound closure in three random fields was quantified.

With the transwell assay, 24-well transwell cell culture chambers (8-µm pores; MilliporeSigma, Burlington, MA, USA) were used; 5×10^4 cells/mL of ARPE-19 cells were suspended in 200 µL of FBS-free medium and then added to the upper inserts, and 500 µL of medium with 10% FBS and M1-MPs or M2-MPs were added to the lower inserts. After incubation with MPs for 8 hours, cells across pores were fixed with 4% paraformaldehyde and stained with 1% crystal violet solution (Beyotime Biotechnology, Haimen, China) for 30 minutes. For each chamber, migrating cells in three random fields were counted.

Western Blot

ARPE-19 cells were lysed by ice-cold radioimmunoprecipitation assay buffer containing protease and phosphatase inhibitor cocktails (Roche, Basel, Switzerland). The extracted proteins were separated by sodium dodecyl sulfate–polyacrylamide gel electrophoresis and transferred to polyvinylidene fluoride membranes (MilliporeSigma). After blocking with 5% skim milk, the membrane was incubated at 4°C overnight with the following primary antibodies: PI3Kp85 (1:1000; Cell Signaling Technology), PTEN (1:1000; Cell Signaling Technology), phosphorylated (p)-AKT (1:1000; Cell Signaling Technology), AKT (1:1000; Cell Signaling Technology), p-mTOR (1:1000; Cell Signaling Technology), mTOR (1:1000; Cell Signaling Technology), pS6 (1:1000; Cell Signaling Technology), S6 (1:1000; Cell Signaling Technology), and GAPDH (1:1000; Utibody, Beijing, China). The membrane was washed and incubated with horseradish peroxidase–linked secondary antibody for 1 hour at room temperature. GAPDH was used as endogenous control, and the proteins band quantification was performed using ImageJ software (National Institutes of Health, Bethesda, MD, USA).

Statistical Analysis

Statistical analysis was performed using Prism 5.0 (GraphPad, San Diego, CA, USA). Quantitative results are displayed as mean ± SD. The statistical significance of differences was calculated with Student's *t*-test or one-way analysis of variance (ANOVA) for multiple comparisons. Differences were considered statistically significant for $P < 0.05$, and the exact *P* values are provided in the text.

Results

Characterization of Microparticles in the Vitreous of Human Patients

To investigate the role of MPs in the pathogenesis of PVR, we isolated MPs from the vitreous from patients with traumatic PVR, patients with RRD complicated with PVR, and control patients. The Table summarizes the demographic and clinical characteristics of the studied patients. Among the study participants, we found that patients with traumatic PVR were significantly younger than patients in the control groups ($P < 0.01$). Compared with the other two groups, traumatic PVR occurred more frequently in male patients ($P < 0.01$). There was no significant difference in the occurrence of systemic diseases, smoking status, or ophthalmology features between the groups.

To understand the role of MPs in the pathogenesis of PVR, we first isolated MPs from the vitreous of the sampled patients and then assessed the MPs by transmission electron microscope (TEM) and nanoparticle tracking analysis. Under the TEM, we found that the isolated MPs appeared as double-layer membrane structures with a diameter between 100 and 1000 nm (Fig. 1A). Furthermore, nanoparticle tracking analysis confirmed that the isolated MPs had a diameter primarily distributed between 100 and 500 nm (Fig. 1B). Next, we determined the expression of cell type–specific markers in isolated vitreous MPs by flow cytometry analysis. Specifically, photoreceptor-derived MPs defined as FITC-PNA^+, microglial-derived MPs defined as FITC-$ILB4^+$, and macrophage-derived MPs defined as CD14-APC^+ were identified (Figs. 1C–1G). Vitreous levels of photoreceptor PNA^+, microglial $ILB4^+$, macrophage $CD14^+$, and Annexin V^+ MPs were markedly increased in patients with traumatic PVR in comparison with control patients ($P = 0.0002$, $P = 0.0012$, $P < 0.0001$, and $P = 0.0003$, respectively) (Fig. 1H, Table) and in patients with RRD complicated with PVR ($P = 0.0042$, $P = 0.0109$, $P = 0.0003$, and $P = 0.0030$, respectively) (Fig. 1H, Table). There was no significant difference in the concentrations of vitreous MPs labeled with PNA^+, ILB^+, $CD14^+$, or Annexin V^+ between patients with RRD with PVR and control patients ($P = 0.5306$, $P = 0.7066$, $P = 0.5406$, and $P = 0.7520$, respectively) (Fig. 1H, Table). In addition, MPs of macrophage origin were further confirmed by dual-labeling with macrophage markers CD14 and CD68. We found that CD14 and CD68 double-positive MPs were significantly higher in patients with traumatic PVR compared with control patients and patients with RRD with PVR ($P = 0.0052$ and $P = 0.0030$, respectively) (Figs. 1I–1L), suggesting increased shedding of MPs from macrophages in patients with traumatic PVR. Altogether, these results indicate that MPs were increased significantly in the vitreous of patients with traumatic PVR, and the increased MPs may have originated from photoreceptors, microglial cells, and macrophages.

Investigative Ophthalmology & Visual Science

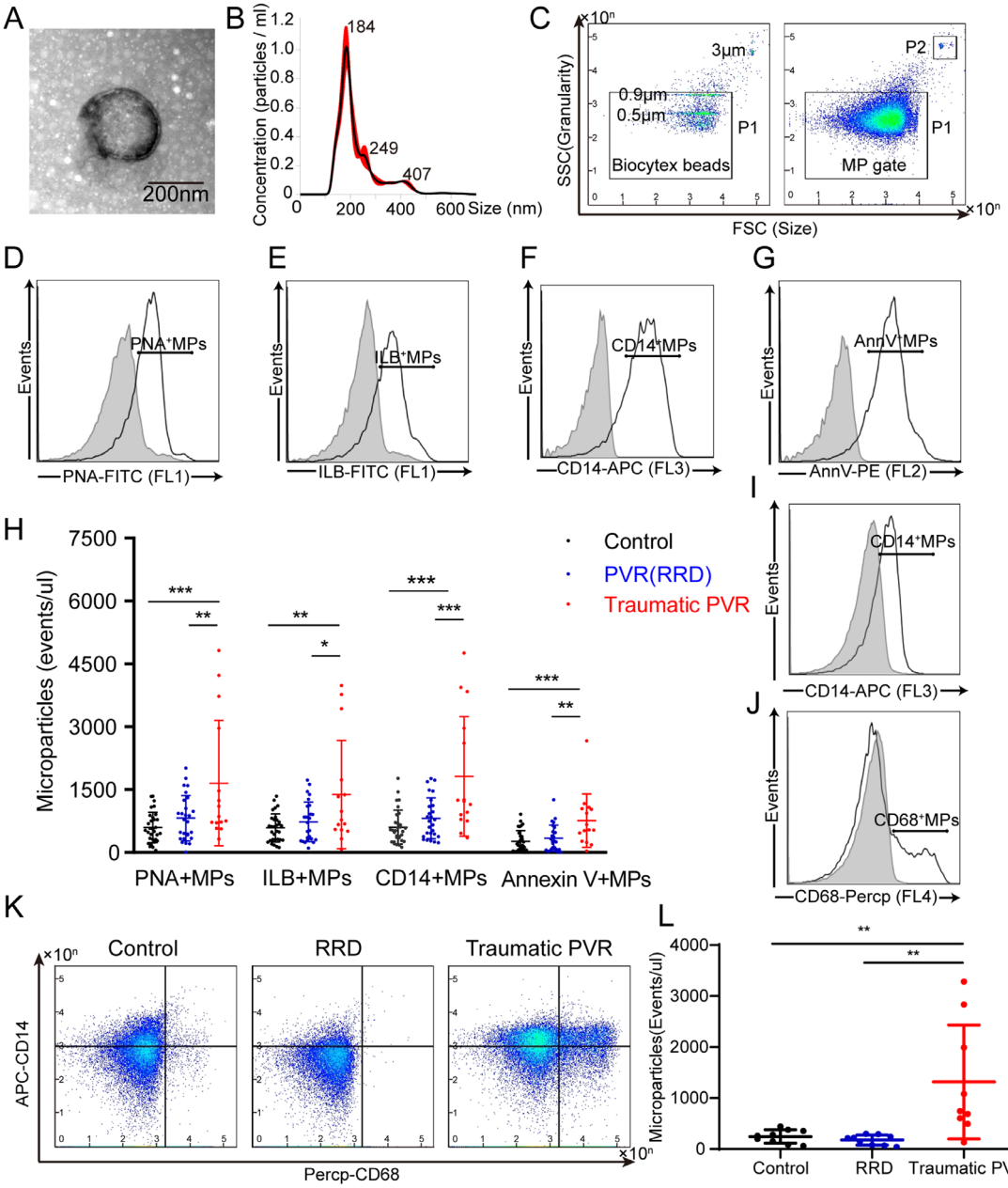

Figure 1. Characterization of MPs in the vitreous of patients with traumatic PVR. (**A**) A TEM was used for ultrastructural analysis of vitreous MPs. (**B**) The size distribution of vitreous MPs was determined with nanoparticle tracking analysis. (**C**) A mix of 0.5-, 0.9-, and 3.0-μm BioCytex beads was ran on forward scatter (FSC) and side scatter (SSC) to set up an acquisition gate (P1) to include particles measuring up to 0.9 μm in diameter. Vitreous samples were run on the same setting to identify all particles ≤ 1 μm in size. MP concentration was assessed by comparison with calibrator beads (P2, 3.5–4.1 μm in diameter) with predetermined concentration. (**D**–**G**) Events selected by size are plotted according to their fluorescence for specific lectin FITC-PNA labeling (**D**), lectin FITC-ILB4 labeling (**E**), anti-human CD14 antibody APC labeling (**F**), or Annexin V PE binding (**G**). *Light-gray areas* represent unspecific binding determined by D-galactose (**D**, **E**), unlabeled isotypic control antibody (**F**), or the absence of calcium (**G**). (**H**) Levels of PNA^+, $ILB4^+$, $CD14^+$, and Annexin V^+ MPs in human vitreous samples measured by flow cytometry. (**I**, **J**) APC-IgG and PerCP-IgG were used as isotype control. (**K**, **L**) Flow cytometry plots and quantification showing $CD14^+$ and $CD68^+$ macrophage-derived MPs in vitreous of control patients and patients with RRD or traumatic PVR ($n = 9$ patients in each group). Values are mean ± SD. $^*P < 0.5$; $^{**}P < 0.1$; $^{***}P < 0.001$ versus control group by one-way ANOVA.

MPs from M2 Polarized Macrophages Are Increased in the Eyes of Patients With Traumatic PVR

Previous studies have identified macrophages as an important risk factor for PVR development.[19,28] In addition, macrophage-derived MPs, especially those derived from M2-phenotype macrophages, showed pathogenic effects in, for example, tumor invasion and fibrogenesis.[29–31] To determine whether the increased macrophage-derived MPs in vitreous samples were of the M1 or M2 phenotype, we performed triple-labeling with the CD68 antibody PerCP (pan-macrophage marker), CD80 antibody PE (M1 macrophage marker), and FITC-CD163 (M2 macrophage marker) of macrophage-derived MPs isolated from control, patients with RRD with PVR, and patients with traumatic

Investigative Ophthalmology & Visual Science

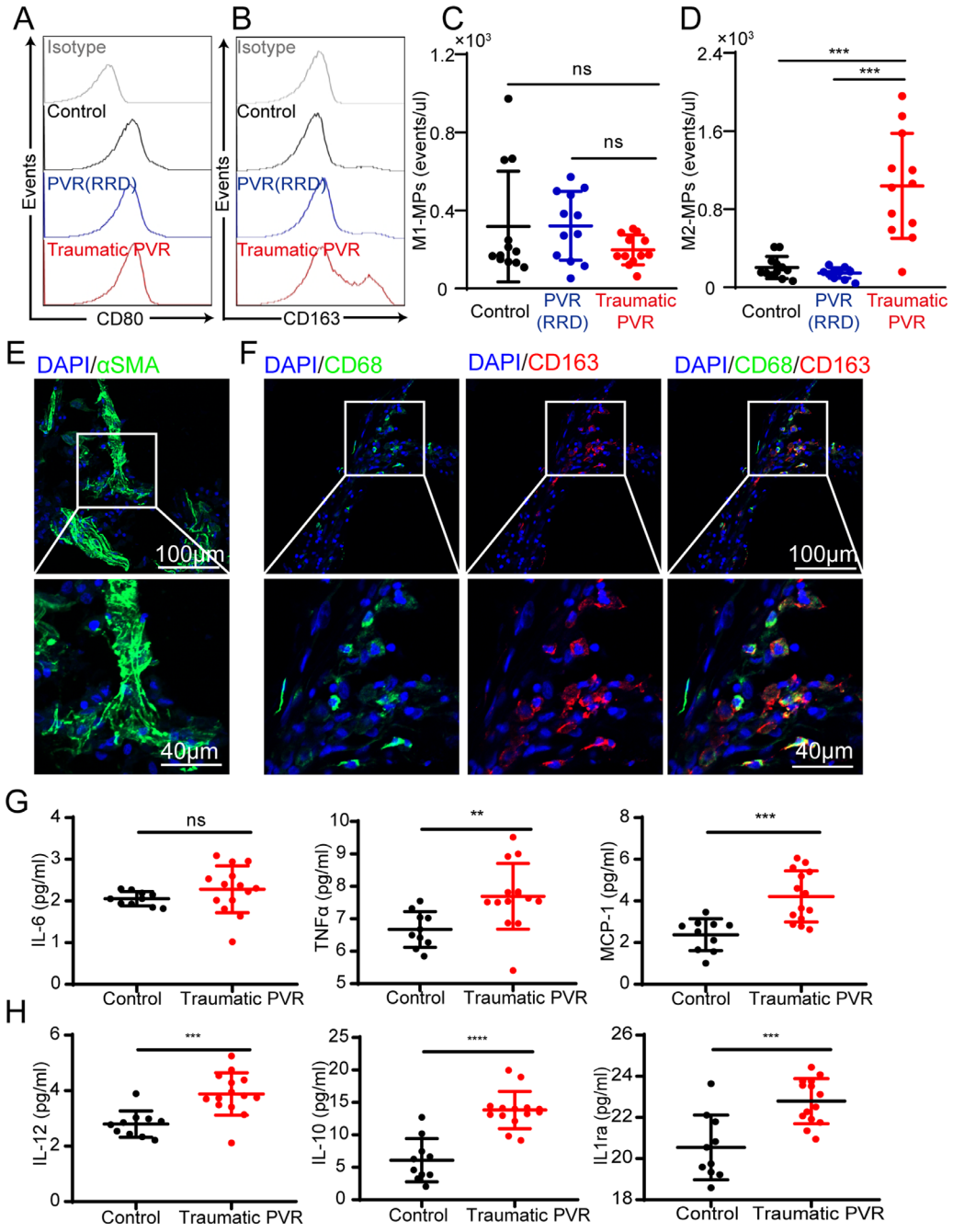

Figure 2. Detection of M2 macrophages and M2-MPs in the eyes of patients with traumatic PVR. (**A**) Flow cytometry histograms of CD68- and CD80-labeled M1-MPs in control patients, patients with RRD with PVR, and patients with traumatic PVR. (B). Flow cytometry histograms of CD68- and CD163-labeled M2-MPs in control patients, patients with RRD with PVR, and patients with traumatic PVR. (**C**) Quantification of vitreous M1-MPs in different groups. (**D**) Quantification of vitreous M2-MPs in different groups ($n = 12$ patients in each group). *Gray lines* represent unstained MPs. (**E**, **F**) Representative confocal images showing expressions of αSMA (**E**) and markers of macrophages (CD68) and M2 polarized macrophages (CD163) (**F**) in epiretinal membranes from patients with traumatic PVR. (**G**, **H**) Vitreous levels of cytokines related to M1 macrophages (**G**) or M2 macrophages (**H**) from control patients and patients with traumatic PVR were measured by ELISA. Values are mean ± SD. $^{*}P < 0.5$; $^{**}P < 0.1$; $^{***}P < 0.001$ versus control group by one-way ANOVA.

PVR. We found M2-MPs, defined as CD68 and CD163 double-positive MPs, were significantly higher in the traumatic PVR group than in the control and RRD with PVR groups ($P < 0.0001$ and $P < 0.0001$, respectively) (Figs. 2B, 2D), whereas no significant difference was observed for M1-MPs, defined as CD68 and CD80 double-positive MPs, in the traumatic PVR group compared with the control and RRD with PVR groups ($P = 0.3116$ and $P = 0.2934$, respectively) (Figs. 2A, 2C).

Next, we examined the presence of M2 polarized macrophages on epiretinal membranes (positive for αSMA) (Fig. 2E) collected from patients with traumatic PVR by immunostaining. We found positive fluorescent signals of CD163 (M2 marker) but not CD86 (M1 marker; data not

Investigative Ophthalmology & Visual Science

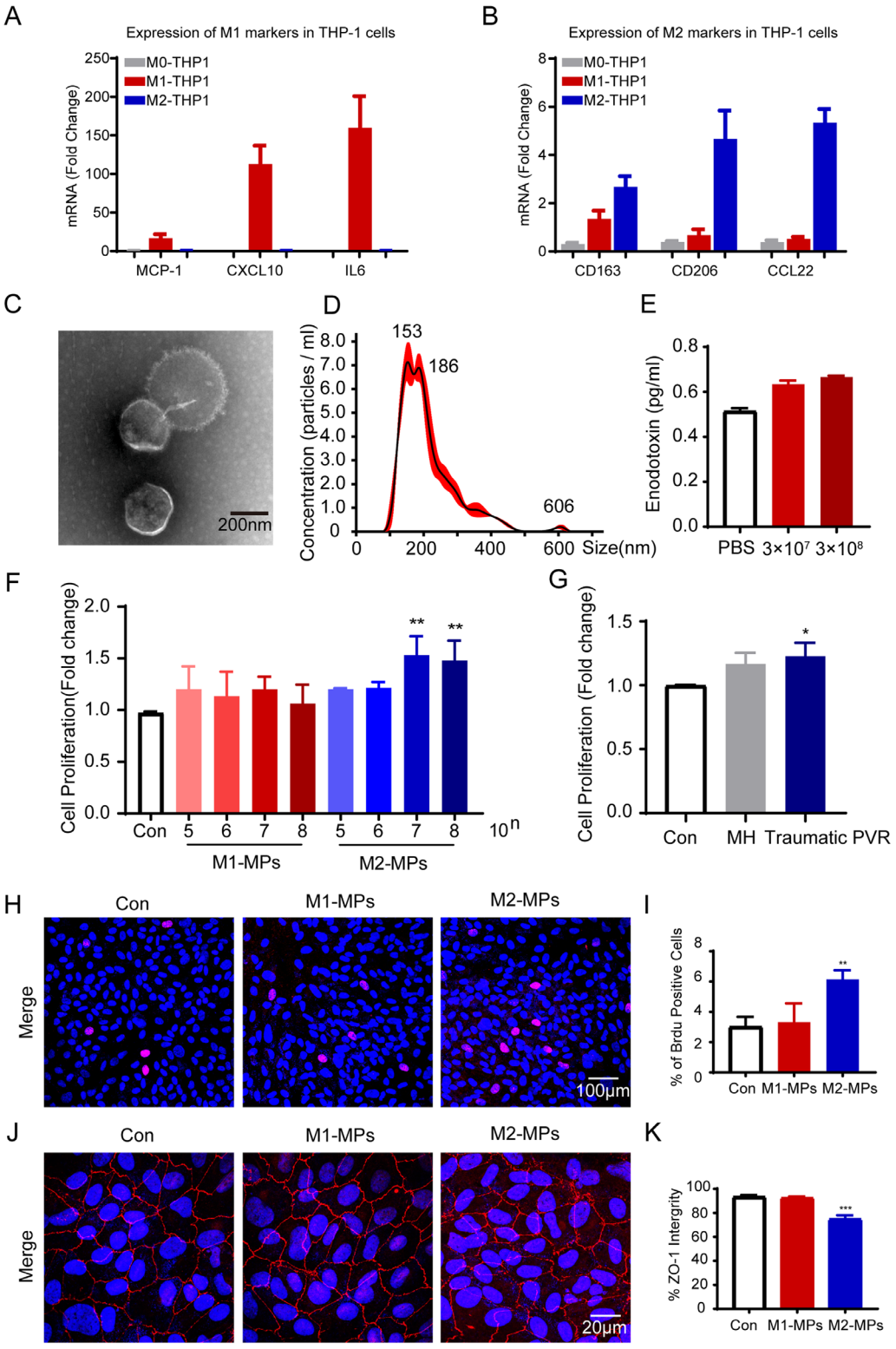

Figure 3. M2-MPs promoted RPE cell proliferation and disrupt the tight junction. Differentiation of monocytic THP-1 cells into M1 and M2 macrophages was stimulated with LPS/IFN-γ and IL-4/IL-13, respectively. (**A**, **B**) mRNA expression of markers of (**A**) M1 macrophages (MCP-1, CXCL10, and IL-6) and (**B**) M2 macrophages (CD163, CD206, and CCL22) in THP-1 cells were detected by RT-PCR. (**C**) Representative TEM image of MPs isolated from aforementioned THP-1 cells conditioned medium. (**D**) Nanoparticle tracking analysis of THP-1 microparticles showing the size distribution to be between 100 and 500 nm with a peak around 200 nm. (**E**) Measurement of endotoxin/LPS levels in M1-MPs using a LPS ELISA kit. (**F**) Measurement of cell proliferation by CCK8 assay in RPE cells treated with THP-1–derived M1-MPs and M2-MPs for 48 hours. (**G**) Measurement of cell proliferation by CCK8 assay in RPE cells treated with vitreous 1×10^7/mL MPs collected from patients with macular hole (MH) and traumatic PVR. (**H**, **I**) Measurement of RPE cell proliferation by the BrdU incorporation assay and quantification. (**J**) Immunostaining of tight-junction protein ZO-1 in ARPE-19 cells treated with M1-MPs or M2-MPs for 48 hours. (**K**) The integrity of ZO-1 proteins was evaluated by calculating the ratio of the continuous tight junction to cell circumference using Image J. Values are mean ± SD from at least three independent experiments. $^{*}P < 0.5$; $^{**}P < 0.1$; $^{***}P < 0.001$ versus control group by one-way ANOVA.

Investigative Ophthalmology & Visual Science

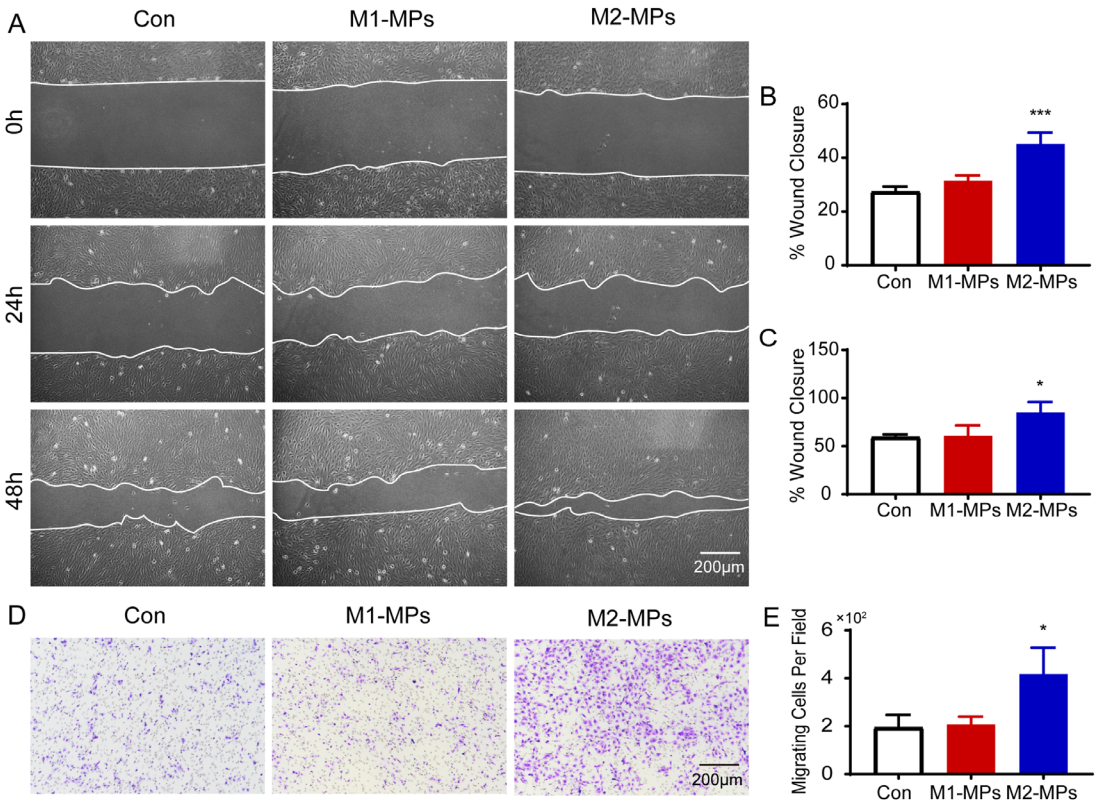

Figure 4. M2-MPs induced ARPE-19 cell migration. (**A**) ARPE-19 cells were treated with 1×10^7/mL M1-MPs or M2-MPs, and cell migration was assessed by scratch assay. (**B**, **C**) Quantification of migrating RPE cells 24 hours (**B**) and 48 hours (**C**) after wound scratch. (**D**) M1-MP–induced and M2-MP–induced migration of RPE cells was confirmed by transwell assay. (**E**) Quantification of the transwell assay. The number of migrating cells was counted at 8 hours after MP treatment. Values are mean ± SD from at least three independent experiments. $^{*}P < 0.5$; $^{**}P < 0.1$; $^{***}P < 0.001$ versus control group by one-way ANOVA.

shown) in the examined epiretinal membranes, colocalizing with pan macrophage marker CD68 (Fig. 2F). M1 or M2 polarized macrophages can be distinguished by differential cytokine production; for example, proinflammatory cytokines such as IL-6, TNF-α, and MCP-1 are associated with M1 macrophages, whereas M2 macrophages produce the anti-inflammatory cytokines IL-10, IL-12, and IL-1ra.[32–34] To further substantiate which macrophage phenotype (M1 vs. M2) was present within the vitreous samples from patients with traumatic PVR and control patients, we evaluated macrophage-induced cytokine production. We found that vitreous levels of TNF-α, MCP-1, IL-10, IL-12, and IL-1ra were significantly higher in the traumatic PVR group than in the control group (Fig. 2G). Among these, the cytokines mostly secreted by M2 macrophages (IL-10, IL-12, and IL-1ra) showed remarkable fold changes in their expression levels compared with the control group (Fig. 2H). There was no significant difference in the vitreous IL-6 expression levels between the two groups (Fig. 2G). Together, our data suggest that M2 macrophages are activated after ocular trauma, accompanied by increased MPs shedding, which is likely involved in the pathogenesis of PVR.

M2-MPs Promote RPE Cell Proliferation and Migration

To further understand the pathogenic role of macrophage-derived MPs in PVR, the effect of macrophage-derived MPs on the RPE EMT was studied in vitro with ARPE-19 cells. However, due to the challenge of the limited amounts of MPs collected from human vitreous samples, we utilized MPs isolated from cultured THP-1 cells for the in vitro study. Successful induction of THP-1 cells into M1 or M2 polarized macrophages was confirmed by qRT-PCR, which showed marked mRNA expression of M1 markers such as *MCP-1*, *IL6*, and *CXCL10* in IFN-γ/LPS–treated THP-1 cells (Fig. 3A) and the M2 markers *CD163*, *CD206*, and *CCL22* in IL-4/IL-13–treated THP-1 cells (Fig. 3B). To this end, we isolated MPs from the differentiated THP-1 cells and confirmed their double-membrane structure with a TEM (Fig. 3C); the size distribution was determined with nanoparticle tracking analysis and was found to be between 100 and 500 nm (Fig. 3D). Because LPS was used to induce M1 polarization, we determined endotoxin levels in M1-MPs and found that the endotoxin levels in M1-MPs were similar to the PBS solvent levels (Fig. 3E), thus ruling out the possibility of LPS contamination in M1-MPs.

Exposure of ARPE-19 cells to M2-MPs at 1×10^7/mL or 1×10^8/mL but not M1-MPs significantly increased cell viability compared with the PBS control ($P = 0.0044$ and $P = 0.0104$, respectively) (Fig. 3F). In addition, vitreous MPs from patients with traumatic PVR also significantly increased RPE cell viability compared with patients with macular hole or control subjects ($P = 0.0231$) (Fig. 3G). The BrdU incorporation assay revealed increased proliferation of RPE cells by M2-MPs compared with control ($P = 0.0053$) (Figs. 3H, 3I), although no such effect was observed in M1-MP–treated cells (Figs. 3H, 3I). The epithelial integrity of ARPE-19 cells was

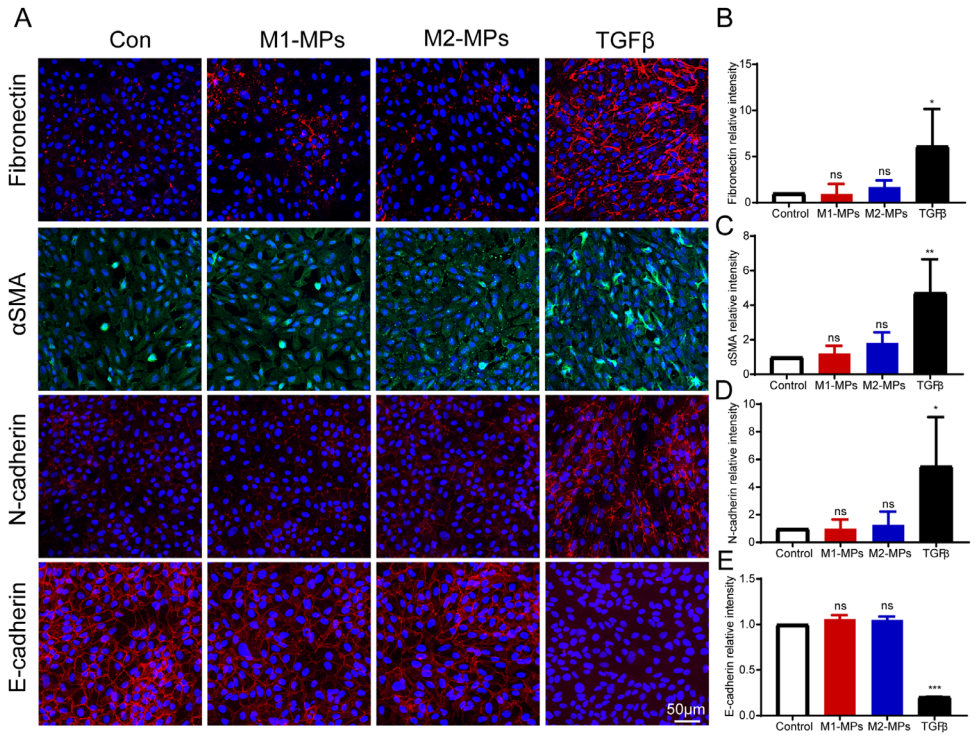

Figure 5. M2-MPs did not affect the fibrotic protein expressions in ARPE-19 cells. (**A**) Immunostaining of fibronectin, αSMA, N-cadherin, and E-cadherin in ARPE-19 cells treated with M1-MPs, M2-MPs, or TGF-β for 48 hours. (**B–E**) Quantification of immunostaining shown in (**A**). Values are mean ± SD from at least three independent experiments. $^{*}P < 0.5$; $^{**}P < 0.1$; $^{***}P < 0.001$ versus control group by one-way ANOVA.

evaluated by staining of junction protein ZO-1. In contrast to the continuous lining of ZO-1 in untreated cells, cells co-cultured with M2-MPs but not M1-MPs demonstrated significantly disrupted ZO-1 expression ($P = 0.0004$) (Figs. 3J, 3K). Moreover, the scratch assay showed an enhanced migratory ability of RPE cells after 24 hours of M2-MP treatment ($P = 0.0007$) (Fig. 4B), which was even more pronounced at 48 hours after M2-MP treatment ($P = 0.0018$) (Figs. 4A–4C). Similarly, with the transwell assay, ARPE-19 cells exhibited a twofold increase in mobility stimulated by M2-MPs as compared with untreated cells ($P = 0.0263$) (Figs. 4D, 4E). The M1-MPs, however, did not show any effect in promoting RPE cell migration in the scratch or transwell assay (Figs. 4A–4E).

To further evaluate the RPE EMT, we detected the expressions of several EMT markers, including fibronectin, αSMA, N-cadherin, and E-cadherin, in RPE cells by immunostaining. Among these, decreased expression of E-cadherin and increased expression of fibronectin, αSMA, and N-cadherin are considered to have occurred during the process of RPE EMT.[35,36] TGF-β was included as a positive control because its role in inducing the RPE EMT has been well reported.[37,38] The results showed that, compared with TGF-β, significantly increased fibronectin, αSMA, and N-cadherin expression, as well as M1-MPs or M2-MPs, did not induce an increased expression of these mesenchymal proteins in ARPE-19 cells. In addition, the expression of epithelial marker E-cadherin was significantly reduced by TGF-β, whereas M1-MPs or M2-MPs did not affect the expression of E-cadherin in ARPE-19 cells (Figs. 5A–5E).

Collectively, these data suggest a role for M2-MPs in promoting RPE cell proliferation, migration, and loss of epithelial integrity, suggesting that vitreous macrophage-derived MPs may contribute to RPE activation and PVR development.

M2-MP–Induced RPE Proliferation and Migration Are Mediated by the PI3K/AKT/mTOR Signaling Pathway

Previous studies have revealed that M2-MPs can modulate tumor cell viability and migration through PI3K/AKT signaling in different cancers.[29,39] To validate the previous findings in RPE cells, we examined the impact of PI3K/AKT signaling activation in ARPE-19 cells after M2-MP treatment. We found significantly increased AKT phosphorylation in ARPE-19 cells at 1, 3, and 6 hours after M2-MP treatment ($P = 0.0220$, $P = 0064$, and $P = 0.0080$, respectively) (Figs. 6A, 6B). mTOR and S6 kinase are important downstream targets of the AKT pathway that regulate key cellular activities such as cell proliferation and protein synthesis.[40,41] Western blotting analysis showed that M2-MP treatment triggered the phosphorylation of S6 at Ser240/244 and Ser235/236 in ARPE-19 cells at 1 hour and 3 hours ($P = 0.0432$ and $P = 0.0026$; $P = 0.0339$ and $P = 0.0031$, respectively) (Figs. 6D, 6E). To determine if M2-MP–induced RPE cell proliferation and migration are mediated by the PI3K/AKT/mTOR pathway, we incubated ARPE-19 cells with the AKT inhibitor MK-2206 together with M2-MPs. We found that treatment with MK-2206 markedly reduced the phosphorylation of AKT and S6 triggered by M2-MPs ($P = 0.0016$, $P = 0.001$, and $P < 0.0001$; $P = 0.0068$, $P = 0.017$, and $P = 0.0005$; $P = 0.0068$, $P = 0.017$, and $P = 0.0005$; $P = 0.0254$, $P = 0.0036$, and $P = 0.0004$, respectively) (Figs. 7B–7D). Furthermore, BrdU and transwell assays showed that treatment with

Investigative Ophthalmology & Visual Science

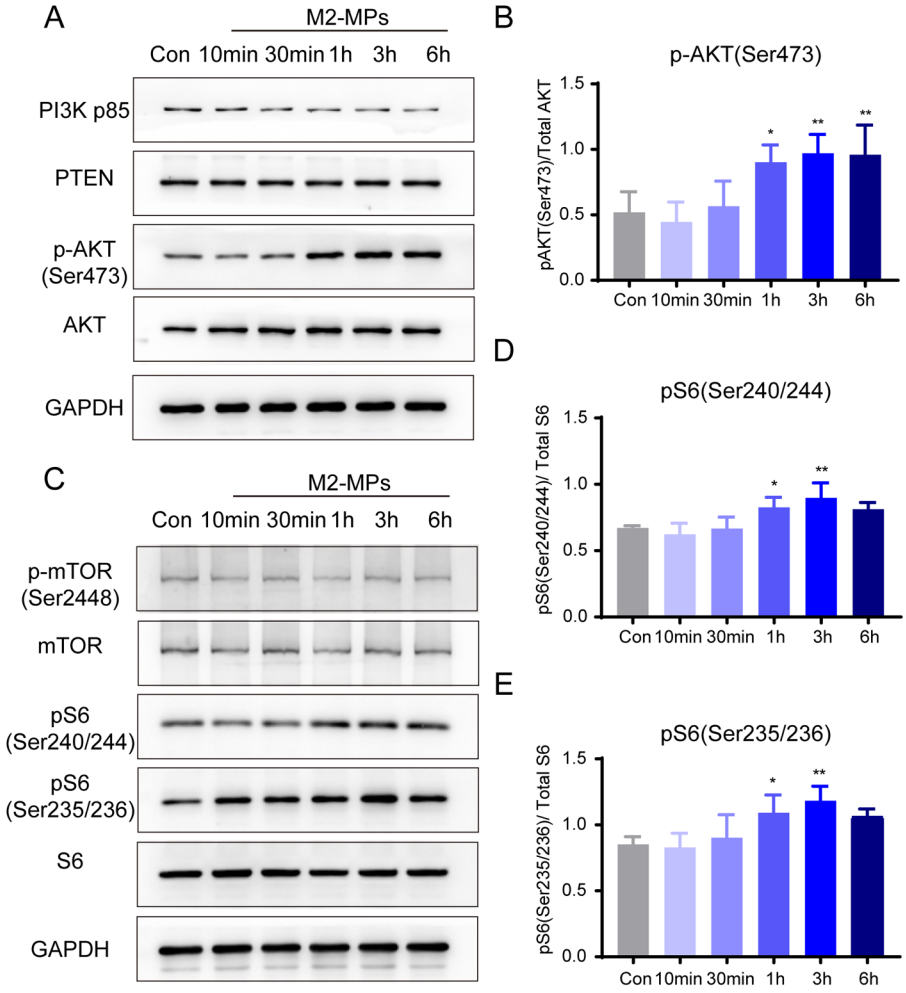

Figure 6. M2-MPs activated the PI3K/AKT/mTOR signaling pathway in ARPE-19 cells. (**A**) Western blot analysis of PI3K, PTEN, p-AKT, and total AKT protein expression in ARPE-19 cells treated with M2-MPs at the indicated time points. (**B**) Quantification of p-AKT expression. (**C**) Western blot analysis of p-mTOR, total mTOR, p-S6, and total S6 in ARPE-19 cells treated with M2-MPs at the indicated time points. (**D**, **E**) Quantification of p-S6 (Ser240/244) (**D**) and p-S6 (Ser235/236) (**E**) expression. Values are mean ± SD from at least three independent experiments. $^{*}P < 0.5$; $^{**}P < 0.1$; $^{***}P < 0.001$ versus control group by one-way ANOVA.

MK-2206 significantly abrogated M2-MP–induced cell proliferation ($P = 0.0006$) (Figs. 7E, 7F) and migration ($P = 0.0009$) in ARPE-19 cells (Figs. 7G–7H). In summary, these results demonstrate that M2-MPs regulate RPE cell proliferation and migration via activation of the PI3K/AKT/mTOR signaling pathway (Fig. 8).

Discussion

In the current study, we have reported for the first time the presence of MPs shedding from photoreceptor cells, microglia cells, and macrophages in the vitreous of patients with traumatic PVR. Moreover, we have demonstrated the presence of M2 polarized macrophages and M2 macrophage-derived MPs in the eyes of traumatic PVR patients. This study thus identified M2-MPs as key stimulators of RPE cell proliferation, migration, and disruptors of tight epithelial junctions through the PI3K/AKT/mTOR signaling pathway, suggesting that vitreous M2-MPs may contribute to the RPE EMT during PVR development (Fig. 8).

Extracellular vesicles (EVs) are membrane vesicles that can be broadly classified into exosomes and microparticles based on their mechanism of biogenesis and size.[42,43] Exosomes are 50- to 150-nm membrane vesicles released to the extracellular environment upon fusion of multivesicular bodies with plasma membrane.[44] Exosomes have shown remarkable potential as a therapeutic delivery vesicle in various ocular diseases, including choroidal neovascularization, diabetic retinopathy, traumatic optic neuropathies, uveal melanoma, and glaucoma.[45–47] Our group recently reported the use of exosomes as carriers to deliver therapeutics into the ocular to treat proliferative retinopathy[48] and traumatic optic neuropathy.[49] In comparison, MPs are 100- to 1000-nm vesicles that bud out into the extracellular space directly from the plasma membrane.[50] MPs have great promise not only as disease biomarkers but also as targets in various diseases, including eye disorders and diseases.[51,52] For example, several studies have reported the involvement of MPs in pathological neoangiogenesis diseases such as DR.[16,53,54] In addition, Tumahai et al.[17] showed that MPs derived from photoreceptors were higher in the vitreous of patients with rhegmatogenous retinal detachment compared with control patients, and photoreceptor-derived MPs may contribute to photoreceptor

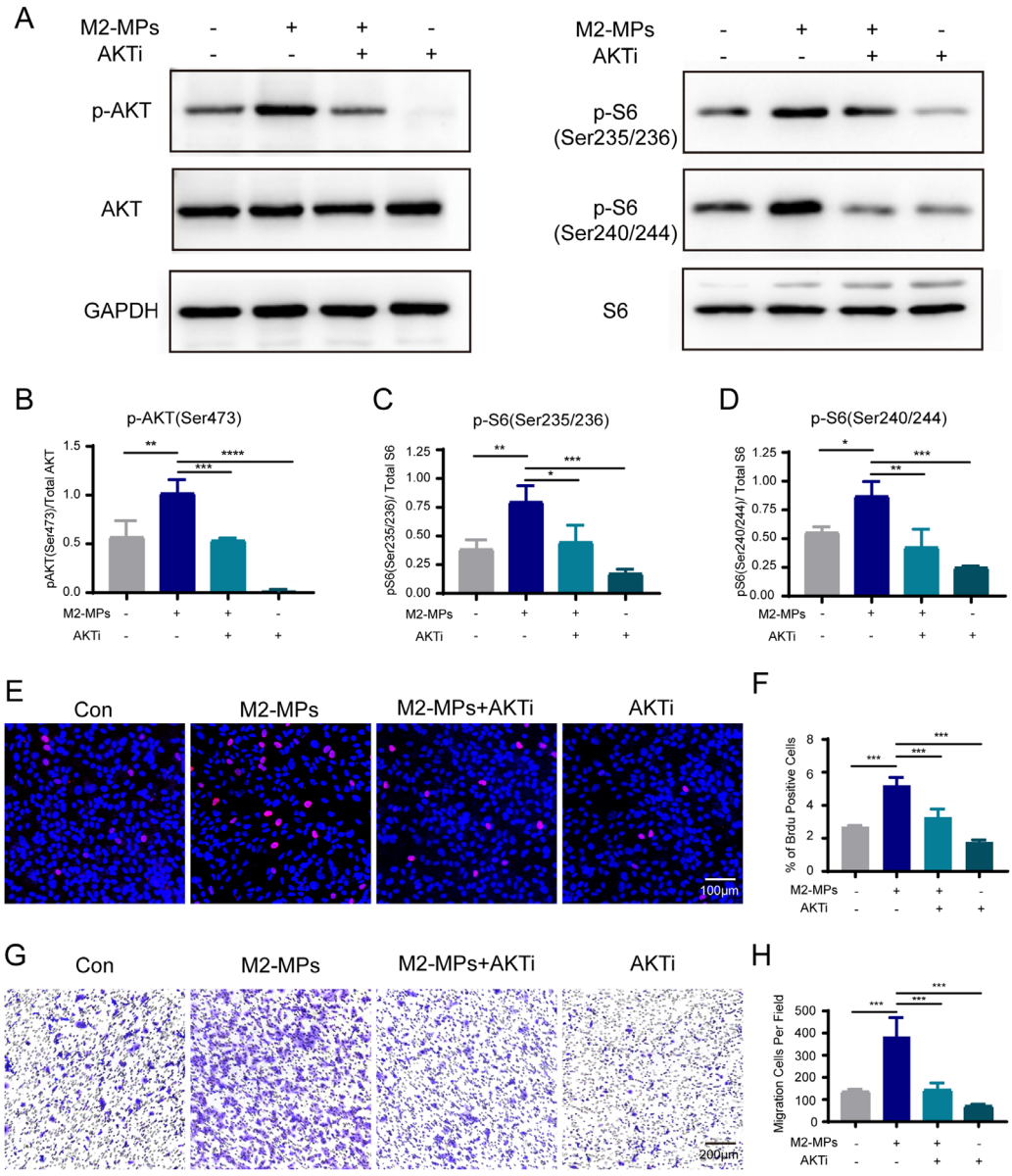

Figure 7. AKT inhibitor prevented M2-MP–induced cell proliferation and migration in ARPE-19 cells. (**A**) Western blot analysis showing that AKT inhibitor MK-2206 mitigated M2-MP–induced phosphorylation of AKT and S6 in ARPE-19 cells. (**B–D**) Quantification of phosphorylation levels for AKT and S6. (**E**) ARPE-19 cells were treated with control, M2-MPs, M2-MPs, and MK-2206 or MK-2206 for 48 hours, then cell proliferation was measured by immunostaining of BrdU for 4 hours. (**F**) Quantification of the BrdU incorporation assay. (**G**) The transwell assay confirmed the effect of M2-MPs and MK-2206 on ARPE-19 cell migration. (**H**) Quantification of the transwell assay. The number of migrating cells was counted at 8 hours after treatment. Values are mean ± SD from at least three independent experiments. $^{*}P < 0.5$; $^{**}P < 0.1$; $^{***}P < 0.001$ versus control group by one-way ANOVA.

apoptosis in patients with rhegmatogenous retinal detachment. In our study, photoreceptor-derived MPs were also markedly increased in the vitreous of patients with traumatic PVR compared with controls, an observation that is consistent with the findings of Tumahai et al.[17] In addition, we found that microglial- and macrophage-derived MPs were also increased in the vitreous of patients with traumatic PVR.

The pathological process of retinal detachment and ocular trauma involves retinal injury, inflammation, and extracellular matrix remodeling, and such cellular activities are known to stimulate the production of MPs.[4,55,56] For example, shortening of photoreceptor outer segments and cell apoptosis observed in retinal injuries such as retinal detachment and ocular trauma may contribute to the release of MPs from activated or apoptotic retinal cells.[17] Moreover, the vitreous hemorrhage that occurs in ocular trauma is usually accompanied by increased migration of macrophages into the vitreous cavity.[1,19] Our study and the study by Tumahai et al.[17] suggest that increased MP shedding in the vitreous could result from the mechanical stress induced by RD or mechanical ocular trauma. Therefore, vitreous MP levels may be related to the severity of the retinal injury and could be used as markers for disease prognosis. In addition, our study and that of Tumahai et al.[17] revealed that, depending on their parental origin, MPs could exert diverse

Investigative Ophthalmology & Visual Science

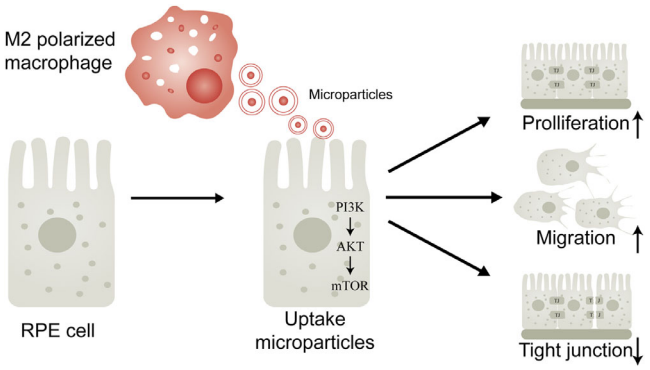

Figure 8. The proposed working model. MPs released by M2 macrophages act on RPE cells, resulting in increased RPE cell migration, proliferation, and disruption of epithelial integrity via activation of PI3K/AKT/mTOR signaling, which may contribute to the progression of traumatic PVR.

biological functions, including inflammation and activation of RPE cells. Thus, this study and others suggest a role for vitreous MPs in the pathogenesis of vitreoretinal disorders.

Upon activation, macrophages can be polarized into the classical activated M1 phenotype or alternative activated M2 phenotype.[16,17] In this study, we found that MPs from M2-polarized macrophages (defined as CD68 and CD163 double-positive MPs) were significantly higher in patients with traumatic PVR than in control patients and patients with RRD with PVR. In addition, the presence of M2 ($CD163^+$) macrophages in the epiretinal membrane may explain the source of increased M2-MPs in the vitreous of patients with traumatic PVR. Moreover, by using M1-MPs and M2-MPs isolated from in vitro polarized THP-1 cells, we demonstrated that M2-MPs but not M1-MPs could stimulate RPE cell proliferation and migration. Our findings are consistent with previous reports showing that M2 macrophage-derived extracellular vesicles promoted the promigratory activity on cancer cells.[7,57] Because the loss of epithelial characteristics and acquisition of mesenchymal phenotype of RPE cells are key pathological events in PVR development,[58] M2-MP–induced RPE cell proliferation, migration, and loss of ZO-1 protein suggest a role for M2-MPs in stimulating the phenotypic transition of RPE cells.

MPs contain a broad range of biological molecules, including proteins, lipids, genetic material, and low-molecular-weight metabolites.[59] The contents of MPs are regulated by their parental origin, environmental factors, cell topography, and activating stimulus.[60,61] The bioactive molecules contained in MPs can modulate the cell signal transduction of recipient cells.[13,62,63] The PI3K/AKT/mTOR signaling pathway has been identified as a critical regulator of numerous cellular processes, including intercellular adhesion, cell proliferation, and migration.[64–67] Here, we have demonstrated that M2-MPs activated PI3K/AKT/mTOR signaling in RPE cells, and AKT inhibitor markedly mitigated M2-MP–induced RPE cell proliferation and migration. However, the bioactive molecules encapsulated in M2-MPs responsible for activating PI3K/AKT/mTOR signaling are unclear. Previous studies showed that exosomes derived from tumor-associated macrophages containing functional apolipoprotein E (ApoE),[29] or microRNA,[68] can promote cancer cell migration by activating AKT signaling. We, however, did not find expressions of ApoE proteins in vitro in polarized M2-MPs. MicroRNA are small, non-coding RNA molecules that function in the posttranscriptional regulation of multiple genes and may be enriched in MPs; whether M2-MPs could modulate AKT signaling via microRNA warrants further investigation.

In this study, we used patients with idiopathic epiretinal membrane samples as control; however, activation of macrophages and microglia cells has been reported during the formation of idiopathic epiretinal membrane.[69,70] Therefore, we cannot exclude the possibility that MPs derived from macrophages and microglia may also be present in the vitreous of patients with idiopathic epiretinal membrane. This was one of the limitations of the current study, and the role of macrophage- and microglia-derived MPs in the idiopathic epiretinal membrane warrants further investigation.

In conclusion, EVs such as MPs and exosomes are emerging as promising tools as disease biomarkers and drug delivery vehicles in various diseases, including ocular disorders and diseases. Our study has highlighted the pathogenic activity of vitreous MPs, especially those of macrophage origin, in proliferative intraocular disorders. Due to the complexity and diversity of EVs, future studies are necessary to expand the scope of EVs biology and pathophysiology, which would greatly benefit the advancement of ocular research and expedite the development of therapeutics in ocular diseases.

Acknowledgments

Supported by grants from the National Natural Science Foundation of China (82020108007, 81830026, 81970828) and Beijing–Tianjin–Hebei Special Project (19JCZDJC64300(Z)).

Disclosure: **Y. Song**, None; **M. Liao**, None; **X. Zhao**, None; **H. Han**, None; **X. Dong**, None; **X. Wang**, None; **M. Du**, None; **H. Yan**, None

References

1. Pastor JC, de la Rua ER, Martin F. Proliferative vitreoretinopathy: risk factors and pathobiology. *Prog Retin Eye Res*. 2002;21:127–144.
2. Schwartz SD, Kreiger AE. Proliferative vitreoretinopathy: a natural history of the fellow eye. *Ophthalmology*. 1998;105:785–788.
3. Shu DY, Lovicu FJ. Myofibroblast transdifferentiation: the dark force in ocular wound healing and fibrosis. *Prog Retin Eye Res*. 2017;60:44–65.
4. Morescalchi F, Duse S, Gambicorti E, Romano MR, Costagliola C, Semeraro F. Proliferative vitreoretinopathy after eye injuries: an overexpression of growth factors and cytokines leading to a retinal keloid. *Mediators Inflamm*. 2013;2013:269787.
5. Tamiya S, Kaplan HJ. Role of epithelial-mesenchymal transition in proliferative vitreoretinopathy. *Exp Eye Res*. 2016;142:26–31.
6. Elner SG, Elner VM, Freeman HM, Tolentino FI, Albert DM. The pathology of anterior (peripheral) proliferative vitreoretinopathy. *Trans Am Ophthalmol Soc*. 1988;86:330–353.
7. Zhang LL, Zhang LF, Shi YB. Down-regulated paxillin suppresses cell proliferation and invasion by inhibiting M2 macrophage polarization in colon cancer. *Biol Chem*. 2018;399:1285–1295.
8. Thery C, Ostrowski M, Segura E. Membrane vesicles as conveyors of immune responses. *Nat Rev Immunol*. 2009;9:581–593.

9. Coleman ML, Sahai EA, Yeo M, Bosch M, Dewar A, Olson MF. Membrane blebbing during apoptosis results from caspase-mediated activation of ROCK I. *Nat Cell Biol*. 2001;3:339–345.
10. Holme PA, Orvim U, Hamers MJ, et al. Shear-induced platelet activation and platelet microparticle formation at blood flow conditions as in arteries with a severe stenosis. *Arterioscler Thromb Vasc Biol*. 1997;17:646–653.
11. Janowska-Wieczorek A, Wysoczynski M, Kijowski J, et al. Microvesicles derived from activated platelets induce metastasis and angiogenesis in lung cancer. *Int J Cancer*. 2005;113:752–760.
12. Mallat Z, Hugel B, Ohan J, Leseche G, Freyssinet JM, Tedgui A. Shed membrane microparticles with procoagulant potential in human atherosclerotic plaques: a role for apoptosis in plaque thrombogenicity. *Circulation*. 1999;99:348–353.
13. Muralidharan-Chari V, Clancy JW, Sedgwick A, D'Souza-Schorey C. Microvesicles: mediators of extracellular communication during cancer progression. *J Cell Sci*. 2010;123:1603–1611.
14. Kornek M, Popov Y, Libermann TA, Afdhal NH, Schuppan D. Human T cell microparticles circulate in blood of hepatitis patients and induce fibrolytic activation of hepatic stellate cells. *Hepatology*. 2011;53:230–242.
15. Geddings JE, Mackman N. Tumor-derived tissue factor-positive microparticles and venous thrombosis in cancer patients. *Blood*. 2013;122:1873–1880.
16. Chahed S, Leroyer AS, Benzerroug M, et al. Increased vitreous shedding of microparticles in proliferative diabetic retinopathy stimulates endothelial proliferation. *Diabetes*. 2010;59:694–701.
17. Tumahai P, Saas P, Ricouard F, et al. Vitreous microparticle shedding in retinal detachment: a prospective comparative study. *Invest Ophthalmol Vis Sci*. 2016;57:40–46.
18. Baudouin C, Hofman P, Brignole F, Bayle J, Loubière R, Gastaud P. Immunocytology of cellular components in vitreous and subretinal fluid from patients with proliferative vitreoretinopathy. *Ophthalmologica*. 1991;203:38–46.
19. Nagasaki H, Shinagawa K, Mochizuki M. Risk factors for proliferative vitreoretinopathy. *Prog Retin Eye Res*. 1998;17:77–98.
20. Biswas SK, Sica A, Lewis CE. Plasticity of macrophage function during tumor progression: regulation by distinct molecular mechanisms. *J Immunol*. 2008;180:2011–2017.
21. Okabe Y. Molecular control of the identity of tissue-resident macrophages. *Int Immunol*. 2018;30:485–491.
22. Zhu X, Shen H, Yin X, et al. Macrophages derived exosomes deliver miR-223 to epithelial ovarian cancer cells to elicit a chemoresistant phenotype. *J Exp Clin Cancer Res*. 2019;38:81.
23. Cheng L, Wang Y, Huang L. Exosomes from M1-polarized macrophages potentiate the cancer vaccine by creating a pro-inflammatory microenvironment in the lymph node. *Mol Ther*. 2017;25:1665–1675.
24. The Retina Society Terminology Committee. The classification of retinal detachment with proliferative vitreoretinopathy. *Ophthalmology*. 1983;90:121–125.
25. van der Vlist EJ, Nolte-'t Hoen EN, Stoorvogel W, Arkesteijn GJ, Wauben MH. Fluorescent labeling of nano-sized vesicles released by cells and subsequent quantitative and qualitative analysis by high-resolution flow cytometry. *Nat Protoc*. 2012;7:1311–1326.
26. Cosenza S, Ruiz M, Toupet K, Jorgensen C, Noel D. Mesenchymal stem cells derived exosomes and microparticles protect cartilage and bone from degradation in osteoarthritis. *Sci Rep*. 2017;7:16214.
27. Szatanek R, Baran J, Siedlar M, Baj-Krzyworzeka M. Isolation of extracellular vesicles: determining the correct approach (review). *Int J Mol Med*. 2015;36:11–17.
28. Esser P, Heimann K, Wiedemann P. Macrophages in proliferative vitreoretinopathy and proliferative diabetic retinopathy: differentiation of subpopulations. *Br J Ophthalmol*. 1993;77:731–733.
29. Zheng P, Luo Q, Wang W, et al. Tumor-associated macrophages-derived exosomes promote the migration of gastric cancer cells by transfer of functional apolipoprotein E. *Cell Death Dis*. 2018;9:434.
30. Walsh KB, Campos B, Hart K, Thakar C, Adeoye O. M2 monocyte microparticles are increased in intracerebral hemorrhage. *J Stroke Cerebrovasc Dis*. 2017;26:2369–2375.
31. Zhan C, Ma CB, Yuan HM, Cao BY, Zhu JJ. Macrophage-derived microvesicles promote proliferation and migration of Schwann cell on peripheral nerve repair. *Biochem Biophys Res Commun*. 2015;468:343–348.
32. Rőszer T. Understanding the mysterious M2 macrophage through activation markers and effector mechanisms. *Mediators Inflamm*. 2015;2015:816460.
33. Duval C, Brien ME, Gaudreault V, et al. Differential effect of LPS and IL-1β in term placental explants. *Placenta*. 2019;75:9–15.
34. Schupp JC, Binder H, Jäger B, et al. Macrophage activation in acute exacerbation of idiopathic pulmonary fibrosis. *PLoS One*. 2015;10:e0116775.
35. Schiff L, Boles NC, Fernandes M, Nachmani B, Gentile R, Blenkinsop TA. P38 inhibition reverses TGFβ1 and TNFα-induced contraction in a model of proliferative vitreoretinopathy. *Commun Biol*. 2019;2:162.
36. Yao H, Ge T, Zhang Y, et al. BMP7 antagonizes proliferative vitreoretinopathy through retinal pigment epithelial fibrosis in vivo and in vitro. *FASEB J*. 2019;33:3212–3224.
37. Yokoyama K, Kimoto K, Itoh Y, et al. The PI3K/Akt pathway mediates the expression of type I collagen induced by TGF-β2 in human retinal pigment epithelial cells. *Graefes Arch Clin Exp Ophthalmol*. 2012;250:15–23.
38. Kimoto K, Nakatsuka K, Matsuo N, Yoshioka H. p38 MAPK mediates the expression of type I collagen induced by TGF-beta 2 in human retinal pigment epithelial cells ARPE-19. *Invest Ophthalmol Vis Sci*. 2004;45:2431–2437.
39. Zheng P, Chen L, Yuan X, et al. Exosomal transfer of tumor-associated macrophage-derived miR-21 confers cisplatin resistance in gastric cancer cells. *J Exp Clin Cancer Res*. 2017;36:53.
40. Sharma V, Sharma AK, Punj V, Priya P. Recent nanotechnological interventions targeting PI3K/Akt/mTOR pathway: a focus on breast cancer. *Semin Cancer Biol*. 2019;59:133–146.
41. Martelli AM, Nyåkern M, Tabellini G, et al. Phosphoinositide 3-kinase/Akt signaling pathway and its therapeutical implications for human acute myeloid leukemia. *Leukemia*. 2006;20:911–928.
42. Bei Y, Das S, Rodosthenous RS, et al. Extracellular vesicles in cardiovascular theranostics. *Theranostics*. 2017;7:4168–4182.
43. Wen C, Seeger RC, Fabbri M, Wang L, Wayne AS, Jong AY. Biological roles and potential applications of immune cell-derived extracellular vesicles. *J Extracell Vesicles*. 2017;6:1400370.
44. Zhang ZG, Buller B, Chopp M. Exosomes - beyond stem cells for restorative therapy in stroke and neurological injury. *Nat Rev Neurol*. 2019;15:193–203.
45. Hajrasouliha AR, Jiang G, Lu Q, et al. Exosomes from retinal astrocytes contain antiangiogenic components that inhibit laser-induced choroidal neovascularization. *J Biol Chem*. 2013;288:28058–28067.
46. Sreekumar PG, Kannan R, Kitamura M, et al. αB crystallin is apically secreted within exosomes by polarized human retinal pigment epithelium and provides neuroprotection to adjacent cells. *PLoS One*. 2010;5:e12578.

Investigative Ophthalmology & Visual Science

47. Mead B, Tomarev S. Bone marrow-derived mesenchymal stem cells-derived exosomes promote survival of retinal ganglion cells through miRNA-dependent mechanisms. *Stem Cells Transl Med*. 2017;6:1273–1285.
48. Dong X, Lei Y, Yu Z, et al. Exosome-mediated delivery of an anti-angiogenic peptide inhibits pathological retinal angiogenesis. *Theranostics*. 2021;11:5107–5126.
49. Wang T, Li Y, Guo M, et al. Exosome-mediated delivery of the neuroprotective peptide PACAP38 promotes retinal ganglion cell survival and axon regeneration in rats with traumatic optic neuropathy. *Front Cell Dev Biol*. 2021;9:659783.
50. Burnier L, Fontana P, Kwak BR, Angelillo-Scherrer A. Cell-derived microparticles in haemostasis and vascular medicine. *Thromb Haemost*. 2009;101:439–451.
51. Stępień E, Kabłak-Ziembicka A, Czyż J, Przewłocki T, Małecki M. Microparticles, not only markers but also a therapeutic target in the early stage of diabetic retinopathy and vascular aging. *Expert Opin Ther Targets*. 2012;16:677–688.
52. Zhang W, Chen S, Liu ML. Pathogenic roles of microvesicles in diabetic retinopathy. *Acta Pharmacol Sin*. 2018;39:1–11.
53. Beltramo E, Lopatina T, Berrone E, et al. Extracellular vesicles derived from mesenchymal stem cells induce features of diabetic retinopathy in vitro. *Acta Diabetol*. 2014;51:1055–1064.
54. Ogata N, Nomura S, Shouzu A, Imaizumi M, Arichi M, Matsumura M. Elevation of monocyte-derived microparticles in patients with diabetic retinopathy. *Diabetes Res Clin Pract*. 2006;73:241–248.
55. Roseblade A, Luk F, Rawling T, Ung A, Grau GE, Bebawy M. Cell-derived microparticles: new targets in the therapeutic management of disease. *J Pharm Pharm Sci*. 2013;16:238–253.
56. Sheremata WA, Jy W, Delgado S, Minagar A, McLarty J, Ahn Y. Interferon-beta1a reduces plasma CD31+ endothelial microparticles (CD31+EMP) in multiple sclerosis. *J Neuroinflammation*. 2006;3:23.
57. Ye Y, Xu Y, Lai Y, et al. Long non-coding RNA cox-2 prevents immune evasion and metastasis of hepatocellular carcinoma by altering M1/M2 macrophage polarization. *J Cell Biochem*. 2018;119:2951–2963.
58. Pastor JC, Rojas J, Pastor-Idoate S, Di Lauro S, Gonzalez-Buendia L, Delgado-Tirado S. Proliferative vitreoretinopathy: a new concept of disease pathogenesis and practical consequences. *Prog Retin Eye Res*. 2016;51:125–155.
59. Mause SF, Weber C. Microparticles: protagonists of a novel communication network for intercellular information exchange. *Circ Res*. 2010;107:1047–1057.
60. Pallet N, Sirois I, Bell C, et al. A comprehensive characterization of membrane vesicles released by autophagic human endothelial cells. *Proteomics*. 2013;13:1108–1120.
61. Bobrie A, Théry C. Exosomes and communication between tumours and the immune system: are all exosomes equal? *Biochem Soc Trans*. 2013;41:263–267.
62. Distler JH, Huber LC, Gay S, Distler O, Pisetsky DS. Microparticles as mediators of cellular cross-talk in inflammatory disease. *Autoimmunity*. 2006;39:683–690.
63. Berckmans RJ, Nieuwland R, Kraan MC, et al. Synovial microparticles from arthritic patients modulate chemokine and cytokine release by synoviocytes. *Arthritis Res Ther*. 2005;7:R536–R544.
64. Polivka J, Jr, Janku F. Molecular targets for cancer therapy in the PI3K/AKT/mTOR pathway. *Pharmacol Ther*. 2014;142:164–175.
65. Keppler-Noreuil KM, Parker VE, Darling TN, Martinez-Agosto JA. Somatic overgrowth disorders of the PI3K/AKT/mTOR pathway & therapeutic strategies. *Am J Med Genet C Semin Med Genet*. 2016;172:402–421.
66. Ersahin T, Tuncbag N, Cetin-Atalay R. The PI3K/AKT/mTOR interactive pathway. *Mol Biosyst*. 2015;11:1946–1954.
67. Yu JS, Cui W. Proliferation, survival and metabolism: the role of PI3K/AKT/mTOR signalling in pluripotency and cell fate determination. *Development*. 2016;143:3050–3060.
68. Zhou Y, Ren H, Dai B, et al. Hepatocellular carcinoma-derived exosomal miRNA-21 contributes to tumor progression by converting hepatocyte stellate cells to cancer-associated fibroblasts. *J Exp Clin Cancer Res*. 2018;37:324.
69. Kono T, Kohno T, Inomata H. Epiretinal membrane formation. Light and electron microscopic study in an experimental rabbit model. *Arch Ophthalmol*. 1995;113:359–363.
70. Baek J, Park HY, Lee JH, et al. Elevated M2 macrophage markers in epiretinal membranes with ectopic inner foveal layers. *Invest Ophthalmol Vis Sci*. 2020;61:19.